THE ASTROPHYSICAL JOURNAL, 345:434–450, 1989 October 1

FURTHER EXPERIMENTAL TESTS OF RELATIVISTIC GRAVITY USING THE BINARY PULSAR PSR 1913+16

J. H. TAYLOR
Joseph Henry Laboratories and Physics Department, Princeton University

AND

J. M. WEISBERG
Physics and Astronomy Department, Carleton College
Received 1989 February 13; accepted 1989 March 24

ABSTRACT

Pulse time-of-arrival observations of the binary pulsar PSR 1913+16 now extend over approximately 14 years. The data are consistent with a straightforward model allowing for the motion of the Earth, special and general relativistic effects within the solar system, dispersive propagation in the interstellar medium, relativistic motion of the pulsar in its orbit, and deterministic spin-down behavior of the pulsar itself. The results show that at the present level of precision, the PSR 1913+16 system can be modeled dynamically as a pair of orbiting point masses. A total of five Keplerian and five "post-Keplerian" orbital parameters can now be determined, most of them with remarkably high precision. The masses of the pulsar and its companion are determined (within general relativity) to be $m_1 = 1.442 \pm 0.003$ and $m_2 = 1.386 \pm 0.003$ times the mass of the Sun, respectively, and the orbit is found to be decaying at a rate equal to 1.01 ± 0.01 times the general relativistic prediction for gravitational radiation damping.

Our results represent the first experimental tests of gravitation theory not restricted to the weak-field, slow-motion limit in which nonlinearities and radiation effects are negligible. The excellent agreement of observation with theory shows conclusively that gravitational radiation exists, at the level predicted by general relativity. We also use the results to calculate improved upper limits on the rate of change of the Newtonian gravitational constant, and the fractional energy density (relative to closure density) of a cosmic background of ultra–low-frequency gravitational radiation. These limits are, respectively, $\dot{G}/G = (1.2 \pm 1.3) \times 10^{-11}$ yr^{-1}, and $\Omega_g < 0.04$ at frequencies 10^{-9} to 10^{-12} Hz.

Subject headings: gravitation — pulsars — radiation mechanisms — relativity — stars: binaries

I. INTRODUCTION

The 8 hour binary pulsar PSR 1913+16 has proved to be an outstanding relativity laboratory, perhaps even surpassing the high expectations held shortly after its discovery (Hulse and Taylor 1975). Observations of its pulse arrival times have provided the data necessary (1) to specify the orbital elements and masses of both the pulsar and the companion star; (2) to determine that the orbit is decaying at precisely the rate expected from the emission of gravitational radiation; (3) to rule out several theories of gravitation; and (4), for the first time, to probe experimentally some details of the solution to the general relativistic two-body problem (Taylor *et al.* 1976; Taylor, Fowler, and McCulloch 1979; Taylor and Weisberg 1982; Weisberg and Taylor 1981, 1984). Interesting applications of the data are still being found: some recent published results include the determination of a new upper limit to $\dot{G}/G$ (the fractional rate of change of the Newtonian gravitational constant; Damour, Gibbons, and Taylor 1988) and the first plausible evidence for gravito-magnetic effects, in the form of geodetic precession of the PSR 1913+16 spin axis (Weisberg, Romani, and Taylor 1989).

The pulsar has now been observed regularly for 14 years, with steadily improving data acquisition equipment and techniques. Parameters describing the system have been derived from least-squares fits of arrival-time data to timing models of increasing sophistication and accuracy (Blandford and Teukolsky 1976; Epstein 1977; Haugan 1985, 1988; Damour and Deruelle 1986). As the time span of available data has lengthened and the quality of the data has improved, we have been able to tighten significantly the constraints on the measured physical parameters. In this paper we provide new determinations of the pulsar and orbital parameters, together with a thorough discussion of errors in the data and their effect on the estimated parameter values.

The plan of our paper is as follows. In § II we describe the techniques used to measure pulse arrival times, along with some details of the data acquisition hardware used for this task since 1974. Section III summarizes the development of the detailed relativistic models used to analyze the data, and § IV describes our implementation of these models in software and presents the results obtained for parameters of the models. Consequences of the parameter values are discussed in § V from a point of view free of any assumptions about the strong-field nature of gravity. Then, in § VI, we discuss the implications in the more restricted circumstance in which general relativity is assumed correct. Section VII summarizes our conclusions and outlines the prospects for further progress.

II. MEASURING TOPOCENTRIC PULSE ARRIVAL TIMES

PSR 1913+16 is a pulsar with short period ($P = 59$ ms), large dispersion measure (DM = 169 cm^{-3} pc), and low flux density ($S = 0.7$ mJy at 1400 MHz). It moves in a binary orbit of short period ($P_b = 7.75$ hr) and high eccentricity ($e = 0.617$), with a maximum speed around 400 km s^{-1}. All of these characteristics make it an unusually difficult pulsar to observe. With a very few exceptions (for example, Lyne and Ritchings

1977; Backer *et al.* 1985), useful observations of PSR 1913+16 have been made only with the benefit of the uniquely high sensitivity of the 305 m telescope of the Arecibo Observatory.[1]

Our observations consist of more than 4480 measurements of pulse arrival times at Arecibo between 1974 September and 1988 July. A consistent procedure has been common to nearly all of the measurements. On a given day, the pulsar is observed for the full tracking range of the telescope, about 2.5 hr. The periodic pulsar waveform is averaged for intervals of about 5 minutes, and the resulting integrated profiles are recorded along with time tags corresponding to the first digitized bin of the average profile and occurring near the midpoint of the integration.

Other details of the observations have varied widely over the 14 years, and a total of 13 distinct combinations of data acquisition equipment have been used. The changes were made in order to take advantage of new feed antennas, new receivers, and enhanced signal processing hardware as they were developed. Most changes occurred during the first 6 years of the experiment, during an era of extensive upgrading of the Arecibo telescope's capabilities. Since 1981, we have taken particular care to minimize changes, and to calibrate the resulting instrumental offsets when changes have been deemed desirable. Most of the timing measurements of PSR 1913+16, and indeed all of those with uncertainties less than 40 μs, have been made since 1981 February.

a) Data Acquisition Systems

Important specifications of the first 11 observing systems, including frequency, bandwidth, effective time resolution, and typical measurement uncertainty, were presented and discussed in an earlier paper (Taylor and Weisberg 1982, hereafter TW). The information is summarized and brought up to date in Table 1. The highest quality data discussed in TW are those recorded with "observing system K," which remained in service until late 1984 and has become known as our "Mark I" observing system. It took advantage of a pair of 2 × 32 × 250 kHz filter-bank spectrometers, the detected outputs of which were sent to a pair of 32 channel de-dispersing circuits (Orsten 1970; Boriakoff 1973). The two de-dispersed output signals, each corresponding to the total power in summed orthogonal polarizations from an 8 MHz bandwidth, were routed to a dual 1024 bin digital signal averager clocked in synchronism with the topocentric pulsar period.

As shown in Table 1, a Mark II system was brought into service in 1984 October. This equipment was designed for optimum performance in timing millisecond pulsars (Rawley 1986; Rawley *et al.* 1987; Rawley, Taylor, and Davis 1988). It makes use of one of the 2 × 32 × 250 kHz filter-bank spectrometers, followed by a bank of 32 concurrently operating signal averagers. The total accepted bandwidth is 8 MHz, only half of that used by the Mark I system. Dispersion delays are removed in software before the 32 single-channel profiles are combined to form a grand average for each 5 minute integration.

In 1988 July we began using a Mark III system which combines some of the advantages of both the Mark I and Mark II approaches. Its signal-averaging hardware is multiplexed to allow concurrent averaging of up to 32 signal channels; its speed is adequate for use with the fastest millisecond pulsars; and, with the help of a new 2 × 32 × 1.25 MHz filter bank, it utilizes the full 40 MHz bandpass of the dual-polarization 22 cm feed of the Arecibo telescope. A disadvantage of the present version of the Mark III system is that its frequency resolution is a relatively poor 1.25 MHz per channel. Consequently, the uncorrectable dispersion smearing is a rather large 630 μs.

In each of the 13 observing systems, the detected pulsar signal was sampled continuously at a constant (or nearly constant) rate, and averaged for 5 minutes in synchronism with the apparent pulsar period. In some of the earliest observations, before the PSR 1913+16 parameters were known well enough to allow an adequate ephemeris to be computed in advance of each observing session, raw data samples were recorded on magnetic tape and the Doppler shifting and synchronous averaging accomplished after the observations were completed. Since 1978.4, the average pulsar waveforms have been accumulated in real time, with a computerized ephemeris and associated hardware adjusting the sampling rate to allow

[1] The Arecibo Observatory is part of the National Astronomy and Ionosphere Center, operated by Cornell University under contract with the National Science Foundation.

TABLE 1

OBSERVING SYSTEMS USED AND SUMMARY OF AVAILABLE DATA

Dates	Frequency (MHz)	Total Bandwidth (MHz)	Frequency Channels	System Noise Temperature (K)	Time Resolution (μs)	TOA Uncertainty (μs)	Number of Observations
A. 1974 Sep–Dec[a]	430	8.0	32	175	5000	275	524
B. 1975 Apr–1976 Nov[b]	430	0.64, 3.2	32	175	2000	310	112
C. 1975 Jun–1976 Feb	430	0.25	1	175	2000	890	75
D. 1976 Nov–Dec[a,b]	430	0.64	32	175	750	155	73
E. 1977 Jul–Aug[b]	430	0.64	32	175	340	150	52
F. 1978 Jun–1981 Feb	430	3.34	504	175	43	75	573
G. 1977 Jul–Aug	1410	8.0	32	80	125	75	57
H. 1977 Dec	1410	8.0	32	80	125	55	72
I. 1978 Mar–Apr[a]	1410	8.0	32	80	125	50	116
J. 1980 Jul–1981 Feb	1410	8.0	32	80, 40	200	85	312
Mark I. 1981 Feb–1984 Dec	1410	16.0	64	40	125	20	1719
Mark II. 1984 Oct–1988 Jul	1408	8.0	32	40	125	31	638
Mark III. 1988 Jul–	1404	40.0	32	40	640	16	159

[a] Raw data samples were recorded on magnetic tape, with signal averaging done afterward in software. All other observations used real-time signal averaging, synchronized by means of a precomputed ephemeris.

[b] Some or all of these observations were made with only one polarization.

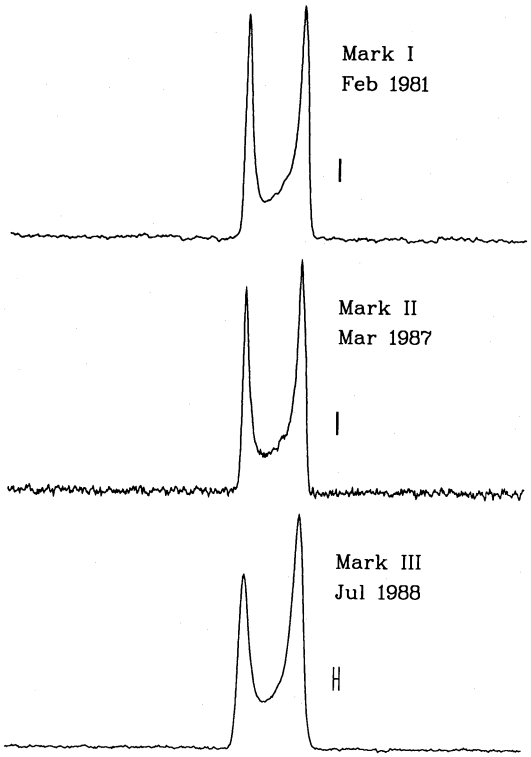

FIG. 1.—Average profiles of PSR 1913+16 as observed with the Mark I, Mark II, and Mark III data acquisition systems at frequencies near 1408 MHz. The effective time resolutions, which are dominated by dispersion smearing, are indicated by bars to the right of each pulse. The full period (59.03 ms) is plotted, and the gradual weakening of component 1 relative to component 2 is a real effect (Weisberg, Romani, and Taylor 1989).

for the small but significant changes in pulsar period during an integration.

Some representative samples of pulse profiles obtained with the pre-1981 observing systems were shown in Figure 1 of TW. These plots illustrated the improvement in time resolution obtained over the first 7 years, as well as the inevitable trade-offs between resolution and signal-to-noise ratio and the significant dependence of pulse shape on frequency. Figure 1 of the present paper shows profiles obtained with the Mark I, Mark II, and Mark III systems at frequencies near 1408 MHz. Each profile is the average of several hundred 5 minute integrations.

b) Determining Times of Arrival and Their Uncertainties

An effective pulse time of arrival (TOA) was calculated for each 5 minute average profile in the following fashion. The observed profile, typically consisting of 1024 numbers representing relative flux density throughout a full pulsar rotation period, was matched with a high signal-to-noise "standard profile" in order to determine the exact phase of the pulsar waveform. This "template matching" was done by least-squares fitting, either in the time domain or in the Fourier transform domain. In either case, a χ^2 "goodness-of-fit" statistic was minimized with respect to three parameters: the level of the baseline, the pulsar signal strength, and the phase offset between observed and standard profiles.

The time delay corresponding to the measured phase was added to the time corresponding to the first bin of the observed profile. In addition, for data acquired since late 1982, a correction (typically amounting to a few microseconds) was applied to the time reckoned by the observatory's master clock, so that the TOA was ultimately referred to Coordinated Universal Time as kept by the US Naval Observatory or the National Institute of Standards and Technology[2] (Davis *et al.* 1985; Rawley *et al.* 1987). The resulting topocentric TOAs, which consitute our basic data set for all further analysis, are specified in units of proper atomic time on Earth, or terrestrial dynamical time (TDT).

We estimate an uncertainty for each TOA as part of the template-matching procedure. Typical values range from a maximum of nearly 1 ms for a small fraction of the early data to 20 μs or less for most of the measurements made since 1981. Because the estimated uncertainties of individual TOAs are themselves subject to significant errors, we improve statistical reliability by using daily average values of uncertainties scaled by the known dependence of telescope gain and system noise temperature on zenith angle.

III. DEVELOPMENT OF THE TIMING MODEL

The phase of a pulsar waveform at a particular time of observation depends on a number of factors, including (1) the spin-down behavior of the pulsar, (2) dispersive delays in the interstellar medium, (3) motion of the Earth within the solar system, (4) orbital motion of the pulsar, if any, and (5) relevant instrumental delays. Analysis of pulsar timing data requires a detailed model of these effects in order to predict the pulsar phases. Differences between predicted and observed values can then be used to determine corrections to various assumed model parameters, as described in § IV.

a) Single Pulsars

An adequate timing model for single pulsars has been developed in stages of increasing accuracy, beginning soon after pulsars were discovered (see, for example, Hunt 1971; Manchester and Peters 1972; Manchester, Taylor, and Van 1974; Manchester and Taylor 1977). Early observations required accuracies only at the 100 μs level; however, the discovery of millisecond pulsars in 1982 made it essential to achieve accuracy in the submicrosecond range. Our current model, embodies in a FORTRAN program called TEMPO, which has been continually evolving since 1972, meets this goal—as proved by extensive tests with 6 years of data from the millisecond pulsar PSR 1937+21. Some details of the model, particularly those not relevant to the orbital motion of binary pulsars, were presented in a paper by Rawley, Taylor, and Davis (1988).

Our timing model for single pulsars is concisely specified in an equation relating the topocentric pulse arrival times t to the corresponding infinite-frequency relativistic coordinate times t_b of pulse arrival at the solar system barycenter (SSB):

$$t_b = t - D/f^2 + (\boldsymbol{r} \cdot \hat{\boldsymbol{n}})/c + \Delta_{E\odot} - \Delta_{S\odot} . \quad (1)$$

In this equation t is measured in the topocentric TDT system, while t_b is in units of barycentric dynamical time (TDB). The observing frequency f is expressed in the rest frame of the SSB; the dispersion constant D, measured in hertz, is conventionally related to the commonly quoted dispersion measure by $D = \mathrm{DM}/(2.41 \times 10^{-16})$. In the remaining terms of equation (1), $\boldsymbol{r}$ is a vector from the SSB to the phase center of the telscope at the time of observation, $\hat{\boldsymbol{n}}$ is a unit vector toward the pulsar, c is the speed of light, $\Delta_{E\odot}$ is the solar system "Einstein delay,"

[2] Formerly the National Bureau of Standards.

or combined effect of gravitational redshift and time dilation due to motions of the Earth and other bodies, and $\Delta_{S\odot}$ is the "Shapiro delay" caused by propagation of the pulsar signal through curved spacetime in the solar system.

The Einstein delay $\Delta_{E\odot}$ amounts to an integral of the expression

$$\frac{d\Delta_{E\odot}}{dt} = \sum_i \frac{Gm_i}{c^2 r_i} + \frac{v_\oplus^2}{2c^2} - \text{constant} . \quad (2)$$

The sum is taken over all significant masses m_i in the solar system, excluding the Earth; r_i is the distance of m_i from Earth; $v_\oplus$ is the velocity of Earth with respect to the SSB; and the additive constant is chosen so that the average value of the right-hand side over a long time interval is equal to zero (for a related discussion see Backer and Hellings 1986).

The Shapiro delay $\Delta_{S\odot}$ is the time-delay analog of the well-known bending of light at the limb of the Sun (Shapiro 1964). Its magnitude is readily computed from the relation

$$\Delta_{S\odot} = -\frac{2GM_\odot}{c^3} \log (1 + \cos \theta) , \quad (3)$$

where $M_\odot$ is the mass of the Sun and θ is the pulsar-Sun-Earth angle at the time of observation; we have neglected the eccentricity of the Earth's orbit. We note in passing that the product $GM_\odot$ is known with higher precision than either G or $M_\odot$ separately; in equation (3) and elsewhere throughout this paper we adopt the constants used in the JPL ephemeris, $GM_\odot = 1.3271243999 \times 10^{26}$ cm^3 s^{-2}, $GM_\odot/c^3 = 4.925490947$ μs, and $c = 2.99792458 \times 10^{10}$ cm s^{-1}.

Accelerations of nonbinary pulsars relative to the SSB are small enough that barycentric dynamical times t_b are equivalent to proper times T in the rest frame of the pulsar, up to an additive constant and a nearly constant Doppler and gravitational redshift scale factor. Therefore, if a pulsar's rotational energy is gradually being dissipated by some deterministic damping mechanism, and the phase is further affected by a stochastic term $\epsilon(T)$, the phase at proper time $T = t_b - t_0$ is given by

$$\phi(T) = \nu T + \tfrac{1}{2}\dot{\nu} T^2 + \tfrac{1}{6}\ddot{\nu} T^3 + \cdots + \epsilon(T) . \quad (4)$$

In this expression $\nu = 1/P$ is the spin frequency, and dots over symbols represent derivatives with respect to time. With a suitable choice of the reference epoch t_0, the calculated phase for a barycentric arrival time $t_b = t_0$ will vanish, and thus t_0 represents a nominal infinite-frequency pulse arrival time at the SSB.

All reasonable dissipation mechanisms yield braking torques proportional to a moderate power of ν, which guarantees that magnitudes of the frequency derivatives decrease rapidly after the first, with $\dot{\nu}/\nu \approx \ddot{\nu}/\dot{\nu}$, and so forth. For PSR 1913+16, the frequency and first derivative are $\nu = 16.9$ s^{-1} and $\dot{\nu} = -2.5 \times 10^{-15}$ s^{-2}, so the expected second derivative is $\ddot{\nu} = 3 \times 10^{-31}$ s^{-3}. Such a small value would be unobservably small over our data span. Moreover, experience has shown (Cordes and Downs 1985) that pulsars with small $\dot{\nu}/\nu$ usually have little or no observable "timing noise"—that is, $\epsilon(T)$ is also very small. Thus there is good reason to expect only the first two terms on the right-hand side of equation (4) to be significant for PSR 1913+16.

b) *Blandford-Teukolsky*

Orbital motion of a pulsar involves significant accelerations. Consequently, the analysis of binary pulsar timing data requires an additional transformation to obtain the proper time T corresponding to each TOA. Blandford and Teukolsky (1976, hereafter BT) derived the first useful formulae for this purpose, soon after the discovery of PSR 1913+16. Their model assumes the orbit to be a slowly precessing Keplerian ellipse in a plane inclined at angle i to the plane of the sky. The pulsar and its companion are assumed to obey essentially Newtonian dynamical laws. The largest short-period relativistic effects—gravitational redshift and time dilation, fully analogous to the Einstein delays within the solar system already discussed—are calculated separately and patched into the model afterward. Any additional effects are accommodated in a phenomenological manner, by allowing for nonzero time derivatives of the orbital elements. Thus, the model is formulated in a way that is free of assumptions about the correct relativistic theory of gravity, and it can be used to detect and measure effects that were not explicitly incorporated at the outset.

In the BT model, the transformation from barycentric arrival time t_b to pulsar proper time T is defined by

$$\begin{aligned} t_b - t_0 = T + \{ & x \sin \omega (\cos E - e) \\ & + [x \cos \omega (1 - e^2)^{1/2} + \gamma] \sin E \} \\ & \times \left\{ 1 - \frac{2\pi}{P_b} [x \cos \omega (1 - e^2)^{1/2} \cos E - x \sin \omega \sin E] \right. \\ & \left. \times (1 - e \cos E)^{-1} \right\} , \end{aligned} \quad (5)$$

where P_b, e, and ω are the binary orbital period, orbital eccentricity, and longitude of periastron; $x \equiv (a_1 \sin i)/c$ is the projected semimajor axis of the pulsar orbit in time units; γ measures the combined effect of gravitational redshift and time dilation; and the eccentric anomaly E is defined by Kepler's equation,

$$E - e \sin E = \frac{2\pi}{P_b} (t_b - T_0) , \quad (6)$$

in which T_0 is a reference time of periastron passage, measured in the TDB system.

Precession of the longitude of periastron is accommodated in the model by setting $\omega = \omega_0 + \dot{\omega}(t_b - T_0)$ in equation (5), and orbital changes caused by gravitational radiation or any other mechanism can be detected and measured by similarly allowing for time derivatives $\dot{P}_b$, $\dot{x}$, and $\dot{e}$. Blandford and Teukolsky (1976) argued that a quasi-Newtonian phenomenological model was an adequate approximation for treating the PSR 1913+16 data available in 1976, and this assertion was borne out in practice (Taylor *et al.* 1976). It is no longer true, however, as shown in § IV, so a better model has become essential for extracting the maximum possible information from the data.

To facilitate discussion in the remainder of § III, we present in Table 2 a list of parameters used in the BT model and in the others we are about to describe. Each model includes right ascension α, declination δ, proper-motion components μ_α and μ_δ, a reference epoch t_0, and the pulsar frequency ν and its derivatives $\dot{\nu}$ and $\ddot{\nu}$. In addition, the models for binary pulsars include the five Keplerian parameters, x, e, T_0, P_b, and ω_0, plus at least two "post-Keplerian" (PK) parameters. Seven orbital parameters are sufficient to specify a binary system completely, up to arbitrary rotations about the line of sight (see, for

TABLE 2

PARAMETERS OF THE TIMING MODELS

Parameter	Single Pulsar	BT Model	EH Model	DD Model	DDGR Model
α	Y	Y	Y	Y	Y
δ	Y	Y	Y	Y	Y
μ_α	Y	Y	Y	Y	Y
μ_δ	Y	Y	Y	Y	Y
t_0	Y	Y	Y	Y	Y
$\nu = 1/P$	Y	Y	Y	Y	Y
$\dot{\nu}$	Y	Y	Y	Y	Y
$\ddot{\nu}$	Y	Y	Y	Y	Y
$x = (a_1 \sin i)/c$	...	Y	Y	Y	Y
e	...	Y	Y	Y	Y
T_0	...	Y	Y	Y	Y
P_b	...	Y	Y	Y	Y
ω_0	...	Y	Y	Y	Y
$\dot{\omega} = 2\pi k/P_b$	...	Y	Y	Y	...
γ	...	Y	Y	Y	...
$\dot{P}_b$	...	Y	Y	Y	...
$s = \sin i$	...	...	Y	Y	...
r	...	...	...	Y	...
$M = m_1 + m_2$	...	...	...	...	Y
m_2	...	...	...	...	Y
$\dot{x}$	...	Y	Y	Y	...
$\dot{e}$	...	Y	Y	Y	...

NOTE.—"Y" denotes inclusion of the parameter in the model.

example, Smarr and Blandford 1976). Additional measurables can therefore yield tests of the nature of gravity or of the "cleanliness" of the binary system. In the BT model, the most significant PK parameters are $\dot{\omega}$, γ, and $\dot{P}_b$, the latter yielding a quantitative test for the existence of gravitational radiation. Secular derivatives $\dot{x}$ and $\dot{e}$ may also be included if desired.

c) *Epstein-Haugan*

More precise observations demand a more accurate timing model, and Epstein (1977, 1979) developed an improved formula that includes the Shapiro time delay in the binary system and the leading short-term periodic terms in the orbital motion. Instead of adding relativistic corrections and phenomenological time derivatives to an otherwise Newtonian treatment of orbital motion, Epstein used the two-body solution found by Wagoner and Will (1976) for the Einstein-Infeld-Hoffmann equation of motion in general relativity. Since the solution closely approximates a precessing ellipse, a description can be made in terms of an osculating orbit whose most significant parameters have the same names as their Keplerian counterparts. Epstein's (1977) equations (A22) and (A16), which we will not reproduce here, define the transformation from t_0 to T in analogy with equations (5) and (6) for the BT model. As shown in Table 2, the gravitational redshift and time dilation parameter γ, and the phenomenological time derivatives, $\dot{\omega}$, $\dot{P}_b$, etc., are also included as in the BT model. An additional free parameter, the orbital projection factor sin i, is added to the model to quantify the post-Newtonian effects.

By 1984, having acquired several years of data with accuracies in the 20 μs range, we discovered that fitting them to the Epstein model produced recognizably nonrandom residuals. At about the same time, Haugan (1985) derived and integrated post-Newtonian equations of motion for a two-body system and compared his results with those of Epstein. This process revealed a flaw in the Epstein model, amounting to the fact that in an eccentric orbit the rate of periastron advance is not constant but rather is modulated by an orbital phase-dependent term. More specifically, the longitude of periastron advances in proportion to the true anomaly rather than the mean anomaly. Haugan derived a corrected version of Epstein's equation (A22) which we used to carry out a satisfactory solution yielding the first direct measurement of sin i (Weisberg and Taylor 1984).

More recently, Haugan (1988, hereafter H88) has recognized (and we have independently proved) that the parameterization used in Epstein (1977) and Haugan (1985) yields a measurement of "sin i" that is principally a test for the presence of the expected periodic modulation of the rate of apsidal advance (which is identical in form, whether caused by relativistic or Newtonian effects) rather than of relativistic orbital-shape and Shapiro-delay effects (for further discussion see Damour and Taylor 1989). Haugan's 1988 paper contains a suggested reparameterization which separates these effects cleanly, and we illustrate the effect of these changes in § IVc.

d) *Damour-Deruelle*

Damour and Deruelle (1986) called attention to another distinguishing aspect of the original Epstein-Haugan (EH) model: it departs in a fundamental way from the theory-independent phenomenological approach of BT. Under the assumption that general relativity correctly describes gravitation in the nonlinear (strong-field) regime, the EH model yields a meaningful estimate of a fourth PK parameter, sin i—and thus a consistency check of the cleanliness of the binary pulsar system as well as a test for gravitational radiation (Weisberg and Taylor 1984). However, the EH parameterization folds several independent effects, the largest of which is not necessarily even relativistic, into the single parameter sin i. If general relativity is not valid under strong-field conditions, the meaning of sin i measured by the EH prescription is unclear. Since no other experimental tests of gravity in strong-field conditions exist, Damour and Deruelle argue persuasively that a more theory-independent approach to the data analysis is highly desirable (see also Damour 1988).

With these ideas in mind, they devised an elegant new method for solving the relativistic two-body problem to post-Newtonian order (Damour and Deruelle 1985). From the solution they derive a new timing formula for binary pulsars (Damour and Deruelle 1986, hereafter DD). This model is valid under very general assumptions about the nature of gravity in strong-field conditions (Damour 1988). The essential transformation relating solar system barycentric time t_b to pulsar proper time T is summarized by the expression

$$t_b - t_0 = T + \Delta_R + \Delta_E + \Delta_S + \Delta_A \,. \tag{7}$$

Here Δ_R, the "Roemer time delay," is the propagation time across the binary orbit, analogous to the solar system term $(\boldsymbol{r} \cdot \hat{\boldsymbol{n}})/c$ in equation (1); Δ_E and Δ_S are the orbital Einstein and Shapiro delays, analogous to $\Delta_{E\odot}$ and $\Delta_{S\odot}$ in the solar system; and Δ_A is a time delay associated with aberration caused by rotation of the pulsar. The Δ's are defined by

$$\Delta_R = x \sin\omega[\cos u - e(1+\delta_r)] + x[1 - e^2(1+\delta_\theta)^2]^{1/2} \cos\omega \sin u \,, \tag{8}$$

$$\Delta_E = \gamma \sin u \,, \tag{9}$$

$$\Delta_S = -2r \log\{1 - e\cos u - s[\sin\omega(\cos u - e) + (1-e^2)^{1/2}\cos\omega \sin u]\} \,, \tag{10}$$

$$\Delta_A = A\{\sin[\omega + A_e(u)] + e\sin\omega\} + B\{\cos[\omega + A_e(u)] + e\cos\omega\} \,, \tag{11}$$

for which one also needs Kepler's equation, the relation between eccentric anomaly u and true anomaly $A_e(u)$, and the time dependence of ω:

$$u - e \sin u = 2\pi\left[\left(\frac{T - T_0}{P_b}\right) - \frac{\dot{P}_b}{2}\left(\frac{T - T_0}{P_b}\right)^2\right], \quad (12)$$

$$A_e(u) = 2 \arctan\left[\left(\frac{1+e}{1-e}\right)^{1/2} \tan\frac{u}{2}\right], \quad (13)$$

$$\omega = \omega_0 + kA_e(u) . \quad (14)$$

As shown in Table 2, the PK parameters of the DD model include $\dot{\omega} \equiv 2\pi k/P_b$, γ, and $\dot{P}_b$, which have essentially the same meanings as in the BT and EH models.[3] In addition, the equation for Δ_S contains two measurable parameters, $s \equiv \sin i$ and r, which characterize the "shape" and "range" of the Shapiro delay. In principle, the small quantities A, B, δ_r, and δ_θ might also be measured. However, as DD point out, these quantities are nearly degenerate with other parameters, and prospects for their measurements appear poor over any reasonable time scale. Their effects are discussed further in the Appendix.

e) *Damour-Deruelle (General Relativity)*

For the sake of completeness, we present one final relativistic timing model for binary pulsars, which we call the DDGR model (Taylor 1987). It amounts to a variation of the DD model in which, contrary to their theory-independent approach, general relativity is explicitly assumed to be the correct theory of gravity. The minimum possible parameter set is used, with two PK parameters—and no ad hoc parameters or extra secular derivatives are introduced. The chosen PK parameters are the total system mass, $M \equiv m_1 + m_2$, and the companion star's mass, m_2 (m_1 is the mass of the pulsar). Equations (8)–(14) remain applicable, but the variables k, γ, $\dot{P}_b$, s, r, A, B, δ_r, and δ_θ, instead of being free (or potentially free) parameters, are determined by the following relations:

$$\frac{a_R^3}{P_b^2} = \frac{GM}{4\pi^2}\left[1 + \left(\frac{m_1 m_2}{M^2} - 9\right)\frac{GM}{2a_R c^2}\right]^2, \quad (15)$$

$$k = \frac{3GM}{c^2 a_R (1 - e^2)}, \quad (16)$$

$$\gamma = \frac{eP_b G m_2 (m_1 + 2m_2)}{2\pi c^2 a_R M}, \quad (17)$$

$$\dot{P}_b = -\frac{192\pi}{5c^5}\left(\frac{2\pi G}{P_b}\right)^{5/3} f(e) m_1 m_2 M^{-1/3}, \quad (18)$$

$$f(e) = (1 + \tfrac{73}{24}e^2 + \tfrac{37}{96}e^4)(1 - e^2)^{-7/2}, \quad (19)$$

$$s = \frac{cxM}{a_R m_2}, \quad (20)$$

$$r = Gm_2/c^3, \quad (21)$$

$$A = \left[\frac{P}{P_b x (1 - e^2)^{1/2}}\right]\left(\frac{a_R m_2}{cM}\right)^2, \quad (22)$$

$$B = 0, \quad (23)$$

$$\delta_r = \frac{G}{c^2 a_R M}(3m_1^2 + 6m_1 m_2 + 2m_2^2), \quad (24)$$

$$\delta_\theta = \frac{G}{c^2 a_R M}\left(\frac{7}{2}m_1^2 + 6m_1 m_2 + 2m_2^2\right). \quad (25)$$

We reemphasize that these equations are specific to general relativity, and for the sake of brevity we have given equations defining the aberration constants A and B that are valid only if the pulsar spin axis is closely aligned with the orbital angular momentum, Further details and references can be found in Damour and Deruelle (1985), DD, and TW.

IV. DETERMINING THE SYSTEM PARAMETERS

a) *Basic Procedure*

Implementation of the four timing models in our computer program TEMPO is a complex but reasonably straightforward process. The program transforms each observed TOA from its topocentric (TDT) value t to a barycentric (TDB) value t_b, using equation (1). The position and velocity of the telescope at the time of an observation are determined by interpolating a solar system ephemeris and correcting, after the fact, for measured irregularities in the rotation rate of the Earth. Earth-rotation data are obtained from the bulletin published by the International Earth Rotation Service, and ephemeris data are taken from either the Center for Astrophysics PEP740R or the Jet Propulsion Laboratory DE200 ephemeris. Both the CfA and the JPL ephemerides are based on numerical integrations of a solar system model whose parameters have been adjusted for best fit to an extensive data base of solar system observations; comparisons between the two (e.g., Prózsyński 1984), as well as our experience in observing millisecond pulsars (Rawley, Taylor, and Davis 1988), confirm that either ephemeris has more than sufficient accuracy for use in analyzing the data from PSR 1913+16. The solar system Einstein delay $\Delta_{E\odot}$ is evaluated by interpolating a table of numerically integrated values included with the CfA ephemeris, or, when the JPL ephemeris is being used, by means of a semi-analytical model developed at the Bureau des Longitudes (BDL) in Paris (Fairhead, Bretagnon, and Lestrade 1988).

The pulsar proper time T is computed from t_b by a process that depends on the binary model being used: equations (5) and (6) are used for the BT model, Haugan's (1985) equations (69) and (71) for the EH model, equations (7)–(14) for the DD model, and equations (7)–(25) for the DDGR model. We call attention to the fact that some of these equations have been presented in the inverse of the form needed. For example, equations (7)–(14) define t_b in terms of T, whereas the opposite is actually required. Some useful short-cut procedures for the necessary inversions are presented in DD.

The pulsar rotational phase $\phi(T_i)$ is determined from equation (4) with $\epsilon = 0$, and a χ^2 statistic measuring goodness of fit of the model to the data is computed from

$$\chi^2 = \sum_{i=1}^{N}\left(\frac{\phi(T_i) - n_i}{\sigma_i/P}\right)^2. \quad (26)$$

In this equation, n_i is the closest integer to each computed $\phi(T_i)$, and σ_i is the estimated uncertainty of T_i (see § IIb). Along with the phases, TEMPO calculates partial derivatives $\partial\phi/\partial\xi|_{T_i}$ with respect to each of the model parameters ξ. These include, in addition to the physical parameters listed in Table 2, up to five instrumental parameters to account for imperfectly calibrated differences between observing systems. Standard

[3] The parameter $\dot{\omega}$ is strictly not the instantaneous rate of change of ω, but rather its average over an orbital period.

linearized techniques (see, for example, Bevington 1969; Press *et al.* 1986) are then used to minimize χ^2 with respect to as many of the model parameters as desired, while others are held fixed. This process requires the evaluation and inversion of a covariance matrix, from which corrections to the estimated parameters and their formal uncertainties are derived.

The integers n_i in equation (26) represent the number of pulsar periods (or rotations of the spinning neutron star) elapsed between each T_i and the reference epoch at which $\phi = 0$. Since imperfect parameter values can lead to ambiguities of whole cycles across gaps in the data, newly discovered binary pulsars require a "bootstrap" procedure in which ambiguities are detected and systematically resolved while the estimated parameter values are being improved (Taylor 1989). For PSR 1913+16 the system parameters have been known well enough since 1975 that no ambiguities have existed. The measured phases $\phi(T_i)$ are typically within ± 0.001 of the neartest integer, even after intervals of a year or more with no observations. It is worth pointing out that the remarkably high precisions for pulsar parameters obtainable from timing observations are largely a result of this ability to connect phase throughout data sets spanning many years.

If the model fitted to the data is an adequate one, and if the data are free of systematic errors, the global minimum of χ^2 should be close to the number of degrees of freedom $N - J$, where J is the number of fitted parameters. In addition, the postfit normalized residuals should have the character of random white noise, with no significant correlations and a Gaussian amplitude distribution, and the formal parameter errors should be realistic estimates of the true uncertainties.

Real data at best approximate such ideals, so it is essential to make quantitative estimates of the size of systematic contributions to the errors. One useful tactic is to study carefully the statistical character of the postfit residuals; another scheme particularly helpful in cases like the present, where subsets of the data have nonuniform quality and may be influenced by different instrumental effects, is to perform solutions in which various subsets of data are intentionally given zero weight. The effect of the unweighted data on the fitted parameter values can then be directly assessed, and their corresponding residuals can give immediate indications of possible systematic errors. We have carried out numerous tests of this kind, and have used them to determine the uncertainty estimates quoted in the next section. Additional details are given in the Appendix.

b) *Astrometric and Spin Parameters*

The first eight items listed in Table 2, the astrometric and spin parameters of the pulsar, are only peripherally related to the main topic of this paper. These parameters depend on annual and secular terms in the timing model, so their values are sensitive to TOA errors that change over long time scales. Consequently, for high-precision measurement of α, δ, ν, $\dot{\nu}$, etc., the frequent changes of data acquisition equipment during 1974–1977 reduce our earliest data to questionable value. The parameter values quoted in Table 3 are based on solutions carried out for data acquired since 1981. For convenience we quote the pulsar spin parameters in terms of both frequency ν and period P.

For several reasons, we list two full sets of results in Table 3. The solution labeled B1950.0 (CfA) is based on the PEP740R ephemeris, including its numerically integrated values for the solar system relativistic clock corrections $\Delta_{E\odot}$. The solution labeled J2000.0 (JPL) is based on the DE200 ephemeris and the BDL semianalytical model for $\Delta_{E\odot}$. For the reference epoch t_0 we list a TDB Julian ephemeris date, roughly centered within our highest quality data, for which $\phi[T(t_0)] = 0$. Thus, t_0 represents a nominal infinite-frequency barycentric pulse arrival time, as well as a reference epoch for the remaining astrometric and spin parameters.

TABLE 3

ASTROMETRIC AND SPIN PARAMETERS OF PSR 1913+16

PARAMETER	COORDINATE SYSTEM	
	B1950.0(CfA)	J2000.0(JPL)
α	$19^h13^m12^s.46549(15)$	$19^h15^m28^s.00018(15)$
δ	16°01′08″.189(3)	16°06′27″.4043(3)
μ_α (mas yr^{-1})	-3.2 ± 1.8	-3.2 ± 1.8
μ_δ (mas yr^{-1})	1.2 ± 2.0	1.2 ± 2.0
ν(s^{-1})	16.940539303217(2)	16.940539303295(2)
$\dot{\nu}(10^{-15}$ s$^{-2})$	−2.47559(2)	−2.47583(2)
$\lvert\ddot{\nu}\rvert(10^{-27}$ s$^{-3})$	<6	<6
t_0(JED 2,445,888+)	0.745517962	0.745517886
P(ms)	59.029997929883(7)	59.029997929613(7)
$\dot{P}(10^{-18}$ s s$^{-1})$	8.62629(8)	8.62713(8)
$\lvert\ddot{P}\rvert(10^{-29}$ s s$^{-1})$	<2	<2

NOTE.—Figures in parentheses are uncertainties in the last digits quoted.

It is known that the coordinate systems of the CfA and JPL ephemerides are not oriented identically (Prószyński 1984; Bartel *et al.* 1985; Backer *et al.* 1985). For this reason, applying any standard recipe (e.g., Standish 1982) to convert the B1950.0 position of PSR 1913+16 to J2000.0 coordinates will not yield exactly the J2000.0 position given in Table 3. Furthermore, our two solutions incorporate different definitions of the unit of time, because they implicitly use different constants for the last term in equation (2). The measured values of ν, $\dot{\nu}$, P, and $\dot{P}$ depend on the value of this constant, and therefore on the time interval over which it was determined. Because the BDL semianalytical model includes cyclic terms with periods up to 1000 yr, while the CfA numerical integration extends over only 50 yr, the BDL model is probably the preferable system to use. We hasten to point put that while these subtleties will be important to others observing PSR 1913+16, both now and in the future, they have no bearing on the remaining results of this paper. Both the CfA and the JPL/BDL systems are good enough descriptions of solar system effects that they have negligible impact on measurement of the orbital parameters.

c) *Orbital Parameters*

We now turn to the orbital parameters of the PSR 1913+16 system, whose measurement and interpretation form the central theme of our paper. A representative set of solutions for the optical parameters is summarized in Tables 4 and 5. For purposes of discussion we include in these tables one solution each for the EH model, the reparameterized Haugan model (H88), and the DDGR model; two for the BT model; and three for the DD model. The first seven solutions are based on the Mark I, Mark II, and Mark III data alone—that is, all of the high-quality data acquired since 1981 February. The last solution, labeled DD(3), includes all data back to 1974 with estimated uncertainties less than about 500 μs. An example of the postfit residuals for solution DD(1) is presented in Figure 2, both as a function of date and as a function of orbital phase.

Table 4 lists values obtained for the five Keplerian orbit parameters. Small but significant differences exist between the BT and other values for x, and between the BT, EH, H88, and

TABLE 4

KEPLERIAN ORBITAL PARAMETERS

Solution	$x = (a_1 \sin i)/c$ (s)	e	T_0 (JED 2,445,888+)	P_b (s)	ω_0 (degrees)
BT(1)	2.341774(9)	0.6171472(10)	0.61724862(8)	27906.980894(2)	220.1426(2)
BT(2)	2.34178(10)	0.6171467(11)	0.61724862(8)	27906.980894(2)	220.143(2)
EH	2.341749(12)	0.617127(5)	0.61724861(8)	27906.980895(2)	220.1428(2)
H88	2.341752(19)	0.617128(6)	0.61724859(10)	27906.980895(2)	220.1428(3)
DDGR	2.341754(9)	0.6171314(10)	0.61724857(7)	27906.980891(2)	220.1428(2)
DD(1)[a]	2.341754(9)	0.6171313(10)	0.61724860(8)	27906.980895(2)	220.1428(2)
DD(2)[a]	2.34176(10)	0.617132(3)	0.6172486(2)	27906.980895(2)	220.143(2)
DD(3)	2.341761(9)	0.6171304(10)	0.61724861(8)	27906.980894(2)	220.1426(2)

NOTE.—Figures in parentheses are uncertainties in the last digits quoted.
[a] Preferred solutions.

remaining values of e. Such differences are to be expected, because the precise definitions of parameters in the three basic models are not identical. Note that we have chosen a reference periastron passage time, T_0, in 1984 July—near the middle of our span of highest quality data—whereas most previously published solutions used a T_0 in 1974 September. The freedom of choice for T_0 arises, of course, from the discrete freedom (modulo 2π) in choosing an origin for the eccentric anomaly in Kepler's equation.

Table 5 lists all of the significantly nonzero PK parameters. Two such parameters exist for the DDGR model, while the BT model has three, EH and H88 each have four, and DD has as many as five [two of which were held fixed in solutions DD(1) and DD(3)]. The remaining columns of Table 5 contain upper limits for $|\dot{x}|$ and $|\dot{e}|$ obtained from the BT(2) and DD(2) solutions, as well as the number of instrumental free parameters, the value of χ^2, and the number of degrees of freedom for all eight solutions.

With the understandable exceptions already mentioned, the solutions yield consistent parameter estimates within the measurement uncertainties. All of the Keplerian parameters are determined to six or more significant figures, as are $\dot{\omega}$ and M, the most important of the PK group.[4] The next most significant PK parameter, γ (or m_2 in the DDGR model), is determined to a fractional accuracy of about 0.2%. The orbital period decay rate, $\dot{P}_b$, is known to 1%, and sin i in the EH model is determined to about 5%. All of these parameters, and the limits for $\dot{x}$ and $\dot{e}$ as well, are readily determined by the linearized least-squares procedure outlined in § IV*a*.

A striking demonstration of the significance of gravitational redshift and time dilation effects in the orbit is produced by setting $\gamma = 0$, minimizing χ^2 with respect to everything else, and comparing the postfit residuals with those produced in a "good" solution in which γ was allowed to vary. Figure 3 shows the results of such a test, directly comparable to the bottom portion of Figure 2. The rapid precession of periastron causes the shape of the orbit delay curve (eqs. [7]–[14]) to change substantially over a few years, yielding large and highly correlated residuals if γ is constrained to zero.

Precession of the periastron and decay of the orbital period also give rise to large effects readily amenable to graphical display. For this purpose, we carried out solutions for each of 19 localized blocks of data, solving for just two parameters, T_0 and ω_0, in each block. The periastron time T_0 was always chosen to corespond to an orbit near the middle of the data segment. All other parameters were held fixed at the values found in the J2000.0 (JPL) solution in Table 3 and the DD(1) solution in Tables 4 and 5. The localized values of T_0 and ω_0 are listed in Table 6 and plotted in Figure 4. To allow error bars to be seen in the figure, we include an expanded-scale version at the bottom in which the expected ω corresponding to the DD(1) parameters has been subtracted. It is obvious that apsidal motion is a huge effect in the PSR 1913+16 system, confirming its strongly relativistic character. The line of apsides of this binary orbit has rotated through nearly 60° during our 14 years of observations.

Figure 5 is a similar graph showing the observable effects of

[4] At the present level of accuracy, it is important to specify that $\dot{\omega}$ is measured in units of degrees per Julian year (365.25 days).

TABLE 5

POST-KEPLERIAN PARAMETERS

Solution	$\dot{\omega}$ (degrees yr^{-1})	γ (ms)	$\dot{P}_b$ (10^{-12})	$s = \sin i$	r (μs)	M ($M_\odot$)	m_2 ($M_\odot$)	$\lvert\dot{x}\rvert$ (10^{-13})	$\lvert\dot{e}\rvert$ (10^{-14} s^{-1})	Instrumental Parameters	χ^2	dof
BT(1)	4.22660(4)	4.288(10)	−2.428(26)	...	...	...	...	0[a]	0[a]	1	2617.8	2500
BT(2)	4.22660(18)	4.29(11)	−2.427(30)	...	...	...	...	<2.7	<4.3	1	2613.3	2498
EH	4.22661(4)	4.281(10)	−2.429(26)	0.73(4)	...	...	...	0[a]	0[a]	1	2551.8	2499
H88	4.22660(4)	4.281(10)	−2.429(27)	$0.71^{+0.06}_{-0.10}$	...	...	...	0[a]	0[a]	1	2551.6	2499
DDGR	...	...	...	...	...	2.82837(4)	1.386(3)	0[a]	0[a]	1	2556.6	2501
DD(1)[b]	4.22659(4)	4.289(10)	−2.427(26)	0.734[a]	6.83[a]	...	...	0[a]	0[a]	1	2552.0	2500
DD(2)[b]	4.22659(18)	4.29(11)	−2.428(34)	[c]	[c]	...	...	<2.4	<1.9	1	2551.9	2496
DD(3)	4.22656(4)	4.296(11)	−2.435(34)	0.734[a]	6.83[a]	...	...	0[a]	0[a]	5	4878.7	4001

NOTE.—Figures in parentheses are uncertainties in the last digits quoted.
[a] Parameter held fixed at this value.
[b] Preferred solutions.
[c] See text and Fig. 7.

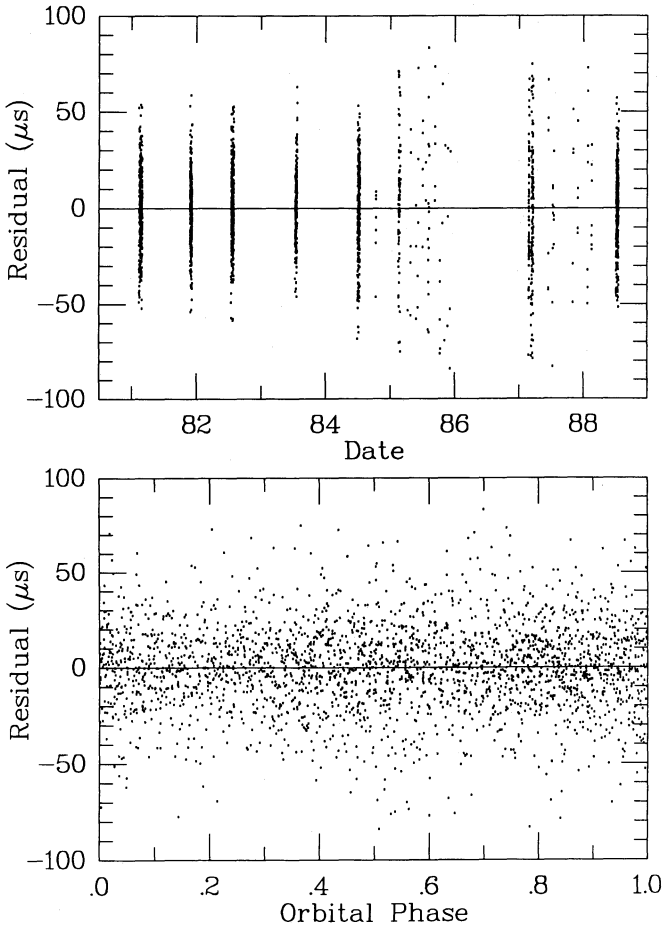

FIG. 2.—Postfit residuals from the DD(1) solution in Tables 4 and 5, plotted separately against date and orbital phase.

TABLE 6

TIMES AND LONGITUDES OF PERIASTRON PASSAGE

Year	T_0 (JED 2,440,000+)	ω_0 (degrees)
1974.78.....	2331.446132(3)	178.983(4)
1974.94.....	2389.585675(2)	179.654(3)
1976.94.....	3118.5909664(19)	188.087(2)
1977.59.....	3356.6401066(18)	190.846(2)
1977.96.....	3493.5910292(11)	192.426(2)
1978.24.....	3593.3972500(6)	193.5845(8)
1978.43.....	3663.487700(2)	194.393(4)
1978.82.....	3807.5445721(9)	196.0622(11)
1979.32.....	3988.4231539(8)	198.1547(9)
1980.11.....	4276.5368946(7)	201.4867(8)
1980.59.....	4455.4774927(7)	203.5581(8)
1981.15.....	4656.38191738(14)	205.88350(15)
1981.92.....	4938.35870602(12)	209.14664(14)
1982.56.....	5172.53186888(11)	211.85639(14)
1983.56.....	5536.55001230(11)	216.06875(14)
1984.52.....	5888.61724869(17)	220.1428(2)
1985.51.....	6249.7284133(4)	224.3214(5)
1987.19.....	6864.0695866(3)	231.4306(5)
1988.54....	7358.57869939(14)	237.1527(2)

NOTE.—Figure in parentheses are uncertainties in the last digits quoted.

orbital decay. The ordinate, measured in seconds and labeled "orbital phase shift," corresponds to the difference between the measured values of T_0 listed in Table 6 and the values that would be expected if there were no dissipative effects in the orbit. Again, as an aid to visualizing the measurement uncertainties, the figure includes an expanded-scale section showing differences between observed and expected periastron times. In the expanded section we also illustrate, with a time origin at

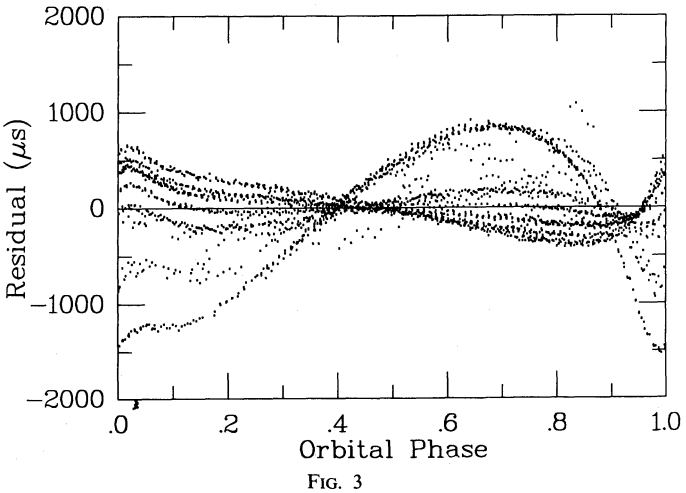

FIG. 3

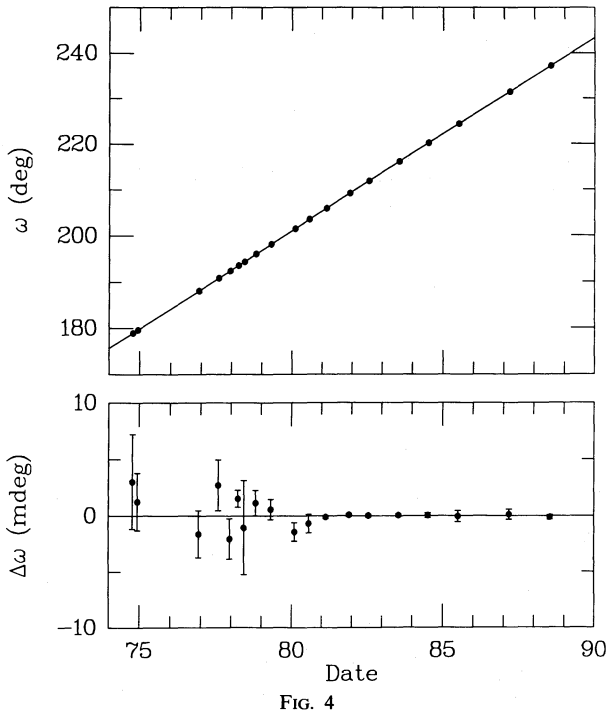

FIG. 4

FIG. 3.—Postfit residuals from a solution similar to DD(1), but constrained by setting $\gamma \equiv 0$ to illustrate the significance of orbital time dilation and gravitational redshift effects. Notice that the vertical scale is 20 times larger than that of Fig. 2.

FIG. 4.—*Top:* Values of the longitude of periastron, ω, measured within 19 localized blocks of data throughout our 14 yr data span. *Bottom:* Differences $\Delta\omega$ between the locally measured values of ω and the values expected according to the DD(1) parameter set.

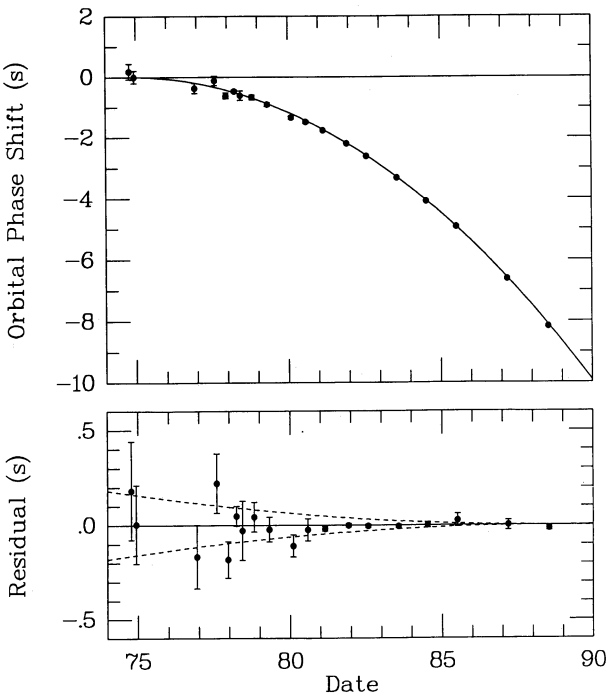

FIG. 5.—*Top:* Cumulative shift of the times of periastron passage relative to a nondissipative model in which the orbital period remains fixed at its 1974.78 value. *Bottom:* Differences between the locally measured periastron times and those expected according to the DD(1) parameter set. Dashed curves illustrate differential trends that would be expected (relative to epoch 1988.54) if the rate of orbital decay $\dot{P}_b$ were 2% larger or 2% smaller.

1988.5, the differential trends that would correspond to 2% larger and 2% smaller values of $\dot{P}_b$. These curves make it clear that the rate of orbital decay can be measured to approximately 1% accuracy with the existing observations.

With the quality of data that we have so far been able to achieve, the values and uncertainties of sin i in the H88 model, and especially s and r in the DD model, cannot be reliably determined by linearized minimization of χ^2. This circumstance occurs because the curvature of the χ^2 hypersurface with respect to these parameters is small enough that, with the present measurement uncertainties, the acceptable zone around the global minimum is larger than the region over which the curvature can be treated as constant. Some important information on the parameters in question can still be obtained, however. A useful strategy is to plot values of $\Delta\chi^2$ with respect to the poorly determined parameters, thereby mapping out the regions around their most likely values.

Such a plot for the H88 solution is shown in Figure 6. It was made by holding sin i fixed at each of the values 0.05, 0.10, ..., 0.95, and minimizing χ^2 with respect to all other model parameters. The global minimum $\chi^2_{\rm min}$ was subtracted from each resulting χ^2(sin i), and the differences interpolated to produce the smooth curve shown. Intervals with $\Delta\chi^2 < 1$ and $\Delta\chi^2 < 4$ formally correspond to 68% and 95% confidence ranges for the single parameter sin i. In Table 5 we quote the 68% or "1 σ" limits.

A map of $\Delta\chi^2(s, r)$ for the DD(2) solution was prepared in a similar way and is reproduced in Figure 7. In this case the list of assumed parameter values is two-dimensional, and the $\Delta\chi^2$ differences were interpolated to facilitate drawing contours by hand. In the figure we use an abscissa linear in cos i rather than sin i, because it is cos i that has a uniform *a priori* distribution, and this helps to illustrate the volume of parameter space excluded by the data. The highest plotted contours, 2.3 and 6.2 units above the minimum, represent the boundaries of nominal 68% and 95% confidence regions for s and r collectively. The contours for $\Delta\chi^2 = 1.0$ and 0.5 have low significance, but help to illustrate where significant contours might fall if higher quality data were available. In the regions to the right of the contours for $\Delta\chi^2 = 6.2$, the value of χ^2 rises very steeply, so that larger values of s and r are quite incompatible with the data. Figure 7 shows that the most likely values of s and r are $s \approx 0.6$ and $r \approx 7$ μs, with uncertainties that are moderately large and interdependent in a complicated way.

V. CONCLUSIONS INDEPENDENT OF A SPECIFIC THEORY OF GRAVITY

a) Astrometry and Rotational Stability

Astrometry of PSR 1913+16 and its surrounding optical field has already been the subject of a number of papers. Taylor, Fowler, and McCulloch (1979) published a pulsar timing position accurate to about 0".1, from which a candidate optical identification was suggested by Crane, Nelson, and Tyson (1979). More recently, Backer *et al.* (1985) measured the pulsar's position with the VLA and presented an updated timing position, based on our data through 1984 July. The two radio positions were shown to be consistent with each other but inconsistent with that of the optical candidate as remeasured by Elliott *et al.* (1980). The position listed in Table 3 is consistent with the earlier timing position (to within 1.8 σ in right ascension and 1.4 σ in declination), and it has considerably smaller uncertainties. It is clear that the optical candidate is an unrelated foreground or background star which happens to lie approximately 0".5 north of the pulsar position. This conclusion is consistent with recent three-color CCD photometry by Boeshaar *et al.* (1988), who conclude that the star is most likely an unassociated dA-K main-sequence field star.

Our solution for the proper motion of PSR 1913+16 is formally quite significant, but for reasons described in the

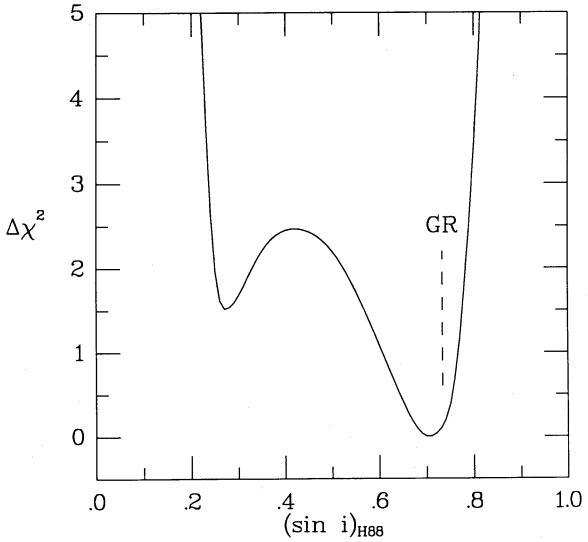

FIG. 6.—The smooth curve represents values of $\Delta\chi^2$ obtained from the H88 solution when sin i was held fixed at a number of values throughout its range. The expected value of sin i according to the DDGR solution—the simplest interpretation of the PSR 1913+16 system within general relativity—is marked by the vertical dashed line.

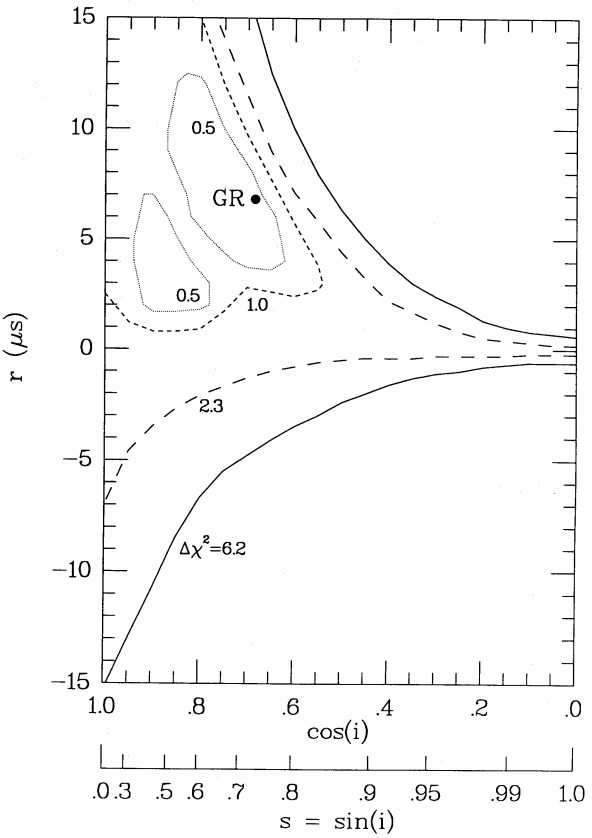

FIG. 7.—Contours of constant $\Delta\chi^2$ in the (s, r)-plane for solution DD(2). Values of s and r corresponding to the DDGR solution are marked by a filled circle.

Appendix we quote it in Table 3 with with conservative estimates of the uncertainties. In Galactic coordinates, the angular motion amounts to to $\mu_l = -0.4 \pm 1.5$, $\mu_b = 3.4 \pm 2.3$ mas y^{-1}. The dispersion measure implies a distance of about 5 kpc (Taylor and Manchester 1981), so the pulsar appears to be moving out of the Galactic plane with a transverse velocity of roughly 80 km s^{-1} in the solar system reference frame. There is not much evidence of the expected effect of Galactic rotation, which should contribute a proper motion toward the Galactic center with $\mu_l \approx -5$ mas yr^{-1} (see Rawley, Taylor, and Davis 1988 and references therein). If the Galactic rotation effect is being canceled by peculiar motion of the pulsar relative to its local neighborhood, the pulsar's total velocity in that frame is at least 140 km s^{-1}, and probably higher when the unknown radial component is included. Models of circumstances surrounding the pulsar's birth strongly suggest velocities of ~150–250 km s^{-1} (Cordes and Wasserman 1984; Burrows and Woosley 1986; Bailes 1988), which would then be consistent with our observations.

The characteristic timing age of PSR 1913+16, $P/\dot{P} = 2 \times 10^8$ yr, is much larger than those for most pulsars, and the surface magnetic field strength, typically estimated from $B = 3 \times 10^{19}(P\dot{P})^{1/2} = 2 \times 10^{10}$ G, is much smaller. We find only marginal evidence for nonzero values of the second derivative and stochastic noise terms of equation (4). As described in the Appendix, attempts to measure such effects over a decade or more, at the extremely low levels of a few milliperiods of accumulated phase, are fraught with difficulties. However, we believe the conservatively stated upper limits for $\ddot{\nu}$ and $\ddot{P}$ quoted in Table 3 to be reliable. The lack of timing noise exceeding ~30 μs over at least 7 years (see Fig. 10 and the Appendix) implies an "activity parameter" $A < -5.7$, making PSR 1913+16 one of the most stable of all known pulsars (Cordes and Downs 1985).

b) *Orbital Dynamics*

It was recognized at the time of discovery of PSR 1913+16 that its orbital elements imply a high-mass, high-velocity binary system containing regions with relativistically strong gravitational fields, and that periastron precession, gravitational redshift, and time dilation should all produce readily measurable effects in its pulse timing data (Hulse and Taylor 1975). Within a few months, many other experimental possibilities had also been suggested, including the long-predicted, but never before observed, gravitational radiation-reaction effects (Esposito and Harrison 1975; Wagoner 1975) and "magnetic" aspects of gravity as experienced by the rapidly spinning pulsar (Damour and Ruffini 1974; Esposito and Harrison 1975; Barker and O'Connell 1975). Most important, the PSR 1913+16 system was seen to offer a first-ever experimental opportunity to probe the nature of gravity in strong-field conditions (Damour 1988; see this paper also for additional references).

As described in §§ III and IV, analysis of PSR 1913+16 timing data according to the DD model yields estimates of five phenomenological PK parameters, three of which are determined to 1% precision or better. Two PK parameters suffice to complete a dynamical specification of the binary system within a particular relativistic theory of gravity. Additional parameters can then be used to provide information on the adequacy of the physical and mathematical models, and—if all else is well—on the gravitational theory in question.

A theory of gravity successfully passing the tests posed by this experiment must account for the well-determined values of $\dot{\omega}$, γ, and $\dot{P}_b$, as well as the limits placed on s, r, $\dot{x}$, and $\dot{e}$. A theory would be in serious trouble if descriptions of the binary system based on different parameter subsets were to lead to conflicting conclusions, such as incompatible estimates of the masses of the two stars. Although a theory might be technically "rescued" by introducing astrophysical complications accompanied by additional free parameters, such ad hoc additions are unlikely to be persuasive unless *all* viable theories of gravity require them.

We call attention to the fact that values of χ^2 for the two BT solutions (see Table 5) are significantly higher than for any of the other fits based on post-1981 data. The relatively poor fit of the BT model to the data is illustrated in Figure 8, in which we have plotted residuals from the BT(2) and DD(1) solutions, in each case averaged into 30 equally spaced bins of orbital phase. The inescapable conclusion is that a Newtonian solution to the gravitational two-body problem, even when retrofitted with Einstein delays and phenomenological time derivatives of the orbital elements, is inadequate to describe the PSR 1913+16 system to the accuracy demanded by our data.

The DD model is the most theory-independent way of characterizing the observed deviations. Our constraints on parameters s and r (Fig. 7) rule out values of s greater than about 0.8 (unless $|r|$ is very small) and negative values of r. Negative values of r are not meaningful, so far as we know, within any theory of gravity. However, they are mathematically permitted by equation (10), so it is reassuring to find that, according to our data, almost certainly $r > 0$. The value of s must lie

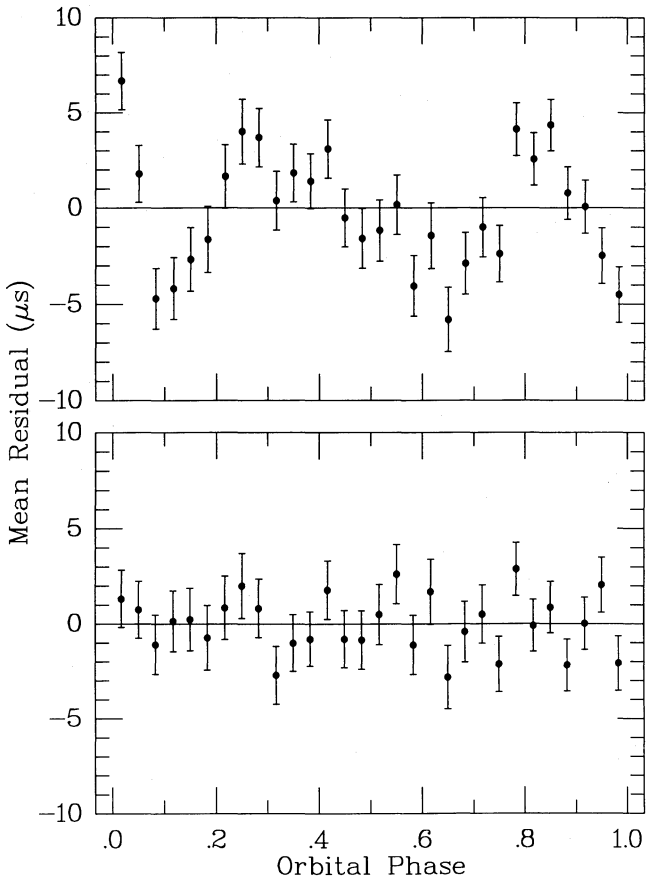

FIG. 8.—Postfit residuals for the BT(2) (*top*) and DD(1) (*bottom*) solutions, averaged into 30 equally spaced bins of orbital phase. The BT model (quasi-Newtonian motion, with "add-on" relativistic effects and time derivatives) is obviously not an adequate approximation.

between zero and one (with suitable definition of ω) for equation (10) to make sense.

VI. CONCLUSIONS BASED ON GENERAL RELATIVITY

We now use the measured orbital parameters to analyze the PSR 1913+16 system under the assumption that general relativity is the correct theory of gravity, at least in the nonquantum regime. Similar treatments within the framework of other theories will be pursued in another paper (Damour and Taylor 1989).

a) Masses of the Two Stars

Table 5 shows that the DDGR solution, with exactly two PK parameters—the minimum number required to specify all of the astrophysical unknowns—has a χ^2 scarcely larger than those of the DD(1), EH, H88, and DD(2) solutions, which have 1, 2, 2, and 5 additional free parameters, respectively. Thus, general relativity successfully accounts for all aspects of our data on the PSR 1913+16 system while using the simplest possible dynamical model: a pair of point masses moving under their mutual gravitational interaction. According to the DDGR solution, the mass of the pulsar is $m_1 = M - m_2 = 1.442 \pm 0.003\ M_\odot$, and the mass of the companion is $m_2 = 1.386 \pm 0.003\ M_\odot$.

The success of general relativity in accounting for our observations is further strengthened by the values of the PK parameters obtained in the H88 and DD solutions. (The EH parameter sin i is not particularly useful in this regard, as mentioned in § IIIc.) As shown for Haugan's model in TW equations (2)–(8), and for the DD model in equations (15)–(25) of § III, a specific value for each PK parameter—together with the well-determined Keplerian orbital elements—specifies a parametric relationship between m_1 and m_2 in general relativity. If Einstein's theory is valid, and the binary system as uncomplicated as our model assumes (see § VI*b*), then the parametric curves should all meet at one point in the (m_1, m_2)-plane.

In practice, experimental uncertainties transform the parametric curves for well-determined parameters into strips of finite width. Contours of $\Delta\chi^2$ for poorly determined parameters like s and r can be mapped into the (m_1, m_2)-plane, as well. Strips and contours for the PSR 1913+16 system in general relativity are plotted in Figure 9. We also plot the curve corresponding to sin $i = 1$. The region below this curve corresponds to sin $i > 1$, and is therefore forbidden.

Notice that the values of m_1 and m_2 determined from the DDGR model, marked with a black dot near the center of the figure, are consistent with *all* of the well-determined parameters, and with the most likely values of $(\sin i)_{H88}$, s, and r as well. For reference, the values of $(\sin i)_{H88}$, s, and r corresponding to the DDGR values of m_1 and m_2 are also marked in Figures 6 and 7. In both cases the nominal general relativity values are close to location of the χ^2 minima. We mention in passing that Damour and Schäfer (1988) have shown that higher order general relativistic effects modify slightly the dependence of M on $\dot{\omega} = 2\pi k/P_b$ (eq. [16]). The corrected value for the total system mass M is $2.82827 + 0.00004\ M_\odot$, smaller than the value given in Table 5 by $0.00010\ M_\odot$. This correction has a negligible effect on the individual masses that

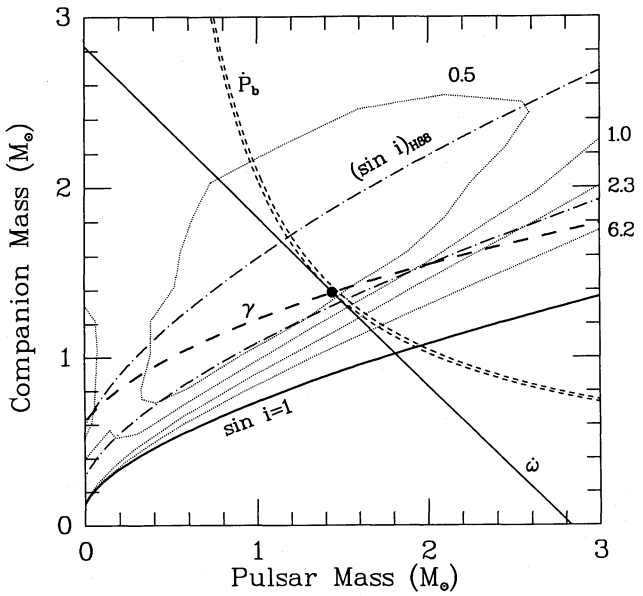

FIG. 9.—Restrictions on the pulsar mass, m_1, and companion mass, m_2, imposed by general relativity are indicated by curves labeled $\dot{\omega}$, γ, $\dot{P}_b$, and $(\sin i)_{H88}$ (the Haugan 1988 sin i parameter). Uncertainties in $\dot{\omega}$ and γ are smaller than the widths of their plotted curves; two curves are plotted for $\dot{P}_b$, and $(\sin i)_{H88}$, bracketing the uncertainty range. Numerically labeled dotted curves represent a mapping of $\Delta\chi^2$ contours for parameters r and s from Fig. 7. Companion masses below the curve labeled sin $i = 1$ are incompatible with the mass function. The point marked with a filled circle corresponds to the mass values given for the DDGR solution in Table 5.

we quote. Note, however, that it illustrates how the high-precision timing of PSR 1913+16 constitutes a new laboratory for relativistic gravity.

b) Astrophysical Considerations

From its discovery, the PSR 1913+16 system has been known to consist most likely of two neutron stars (Hulse and Taylor 1975; Webbink 1975; Smarr and Blandford 1976). Alternative possibilities have been thoroughly explored, and the results have always led to either theoretical or observational difficulties. For example, a white dwarf companion with $m_2 = 1.386\ M_\odot$ would be barely stable, since its mass is precariously close to the Chandrasekhar limit; in any event, it seems impossible for close binary evolution to leave a white dwarf in the system without also circularizing the orbit (Srinivasan and van den Heuvel 1982; van den Heuvel 1987, and references therein). The stripped helium core of a post–main-sequence secondary would probably be visible (Crane, Nelson, and Tyson 1979), but, as we described in § V*a*, no visible counterpart has been found. In short, all models of the system involving white dwarf or helium star companions appear to be highly contrived and therefore unlikely.

Almost certainly, then, both components of the PSR 1913+16 system are neutron stars. In that case, Smarr and Blandford (1976) and others have shown that nonrelativistic contributions to $\dot{\omega}$ and $\dot{P}_b$ are utterly negligible. Burrows and Woosley (1986) have emphasized that the "baryonic masses" of the neutron stars are 10%–15% larger than the gravitational masses we measure, the difference having been carried off by neutrinos emitted during final collapse of the supernova cores. The measured parameters leave only a moderate amount of freedom in many details of the system's evolution (Cordes and Wasserman 1984; Burrows and Woosley 1986). Both the pulsar and the companion, for example, are too heavy to have been formed by accretion of matter onto a white dwarf. The system probably evolved from two massive stars with main-sequence masses between 16 and 18 $M_\odot$, and a small degree of asymmetry in the second supernova explosion is needed to keep the orbit bound with the observed eccentricity.

c) Gravitational Radiation

Substituting $M = 2.82827 \pm 0.00004\ M_\odot$, $m_2 = 1.442 \pm 0.003\ M_\odot$, and the Keplerian parameter in equations (18) and (19) yields the prediction of general relativity for the rate of orbital period change due to gravitational radiation. The result is $(-2.40216 \pm 0.00021) \times 10^{-12}$, in excellent accord with our measured value $(-2.427 \pm 0.026) \times 10^{-12}$. The uncertainty in the theoretical value is dominated by the uncertainty in m_2. We hasten to point out that the six different values of $\dot{P}_b$ listed in Table 5 are in no sense independent estimates, since they all depend on the same observations. It is *not* significant that all six measurements are approximately 1 σ lower than the theoretical value of $\dot{P}_b$.

Equations (18) and (19) were first derived by Peters and Mathews (1963), heuristically starting from a "quadrupole formula" dating back to Einstein (1918; see also Landau and Lifshitz 1962). More rigorous and more complete derivations of the gravitational radiation energy flux, or directly of the observable rate of orbital period change in binary systems of strongly self-gravitating bodies, have been actively pursued in recent years, especially after the announcement of the measurement of $\dot{P}_b$ in PSR 1913+16 (Taylor, Fowler, and McCulloch 1979). The results of these studies have confirmed the validity of equations (18) and (19); for reviews of recent work and references see Will (1986) and Damour (1987). Blanchet and Damour (1989) and Blanchet and Shäfer (1989) have investigated the gravitational radiation loss contributions from terms of higher order in (v/c). Blanchet and Schäfer (1989) find that the fractional error in equation (18), caused by ignoring higher order terms, is only 2.15×10^{-5}, which is negligible at present levels of accuracy.

Our test for gravitational radiation in general relativity can be summarized by the ratio of observed to expected orbital decay rates,

$$\frac{\dot{P}_b(\text{observed})}{\dot{P}_b(\text{theory})} = 1.010 \pm 0.011\ . \tag{27}$$

To the best of our knowledge, there are no other plausible candidates for contributions to $\dot{P}_b$ as large as 1% of the gravitational radiation value. Three of the closest possibilities—transverse motion of the system, Galactic acceleration, and mass-energy loss caused by pulsar spin-down—each probably contribute no more than a few tenths of 1% of the measured effect (Shapiro and Terzian 1976; Will 1981). Thus the 1% agreement is an impressive confirmation of Einstein's theory and, more specifically, a verification of its ability to predict effects involving strong and rapidly varying gravitational fields.

d) The Newtonian Constant G

Damour, Gibbons, and Taylor (1988) have shown that the good agreement between the measured value $\dot{P}_b$ and the general relativistic prediction can be used to place a stringent limit on the rate of change of the Newtonian gravitation constant. Recent interest in Kaluza-Klein and superstring theories has brought renewed interest in possible variation of fundamental coupling constants, because these theories predict changes on the time scale of the Hubble expansion. Our improved precision for $\dot{P}_b$ now allows us to tighten the limit even further. If $\delta\dot{P}_b = \dot{P}_b(\text{observed}) - \dot{P}_b(\text{theory})$, the relevant equation and the new limit can be written as

$$\frac{\dot{G}}{G} = -\frac{\delta\dot{P}_b}{2P_b} = (1.2 \pm 1.3) \times 10^{-11}\ \text{yr}^{-1}\ . \tag{28}$$

This limit is comparable to those obtained from active radar ranging data between Earth and the Viking landers on Mars (Hellings *et al.* 1983; Reasenberg 1983). Further details may be found in the paper by Damour, Gibbons, and Taylor (1988).

e) Ultra–Low-Frequency Gravitational Radiation

Alternatively, the difference between observed and theoretical values of $\dot{P}_b$ can be used to place an upper limit on Ω_g, the energy density of ultra–low-frequency gravitational radiation expressed as a fraction of closure density. Bertotti, Carr, and Rees (1983) show that gravitational waves with periods greater than the span of the observations, but less than the light-travel time to PSR 1913+16, would manifest themselves as an extra contribution to $\delta\dot{P}_b$. The resulting limit on Ω_g can be written as

$$\Omega_g < \frac{1}{2}\left(\frac{\delta\dot{P}_b}{P_b H_0}\right)^2 = 0.04h^{-2}\ , \tag{29}$$

where $H_0 = 100h$ km s^{-1} Mpc^{-1} is the Hubble constant. At the ultra-low frequencies of 10^{-9} to 10^{-12} Hz, this limit is the best available constraint on a stochastic gravitational wave background.

VII. SUMMARY AND PROSPECTS

Accurate time-of-arrival measurements of pulses from the binary pulsar PSR 1913+16 over the last 14 years have enabled us to measure five Keplerian and five post-Keplerian orbital elements, all but two of them with precisions of 1% or better. The evidence indicates that both stellar components are collapsed objects and may be considered point masses in the orbital analysis. Within general relativity, the component masses have been determined with an accuracy of about 0.2%. The orbit is losing energy within 1% of the rate predicted for gravitational radiation damping in general relativity—which we interpret as inconvertible evidence for the existence of gravitational waves. Moreover, the excellent agreement between predicted and observed orbital decay rates provides a limit comparable to the best available for the rate of change of the Newtonian gravitation constant G, and the best available limit on the energy density of a cosmic gravitational wave background at ultra-low frequencies below 10^{-9} Hz.

In another paper (Damour and Taylor 1989), we will explore the fates of several other theories of gravity when their strong-field consequences are used to interpret the parameters of the PSR 1913+16 system. Future observations with 10 times better precision would enable measurements of the post-Keplerian parameters s and r with accuracies around 5%. This is a very exciting prospect because of the considerably tightened constraints that they would place on gravitational theories. Such observations would be feasible with the Arecibo telescope if it were upgraded according to current plans.

The data for this experiment could not have been obtained without the dedication and skills of many individuals at the Arecibo Observatory. We are also most grateful for early work by R. A. Hulse, L. A. Fowler, and P. M. McCulloch, and for essential contributions to the Mark II and Mark III data acquisition systems by L. A. Rawley, D. R. Stinebring, and T. H. Hankins. We have benefited enormously from correspondence and conversations with M. P. Haugan and especially T. Damour, who also provided a critical reading of this manuscript. R. N. Manchester and D. Nice have contributed importantly to the development of TEMPO, and J. F. Chandler and E. M. Standish furnished the CfA and JPL ephemeris data. Our work has been supported financially by a number of grants from the National Science Foundation.

APPENDIX

ANALYSIS OF EXPERIMENTAL ERRORS

Uncertainties for the parameters listed in Tables 3–6 are a combination of our best estimates of both random and systematic errors, and are intended to represent (probably conservative) 1 σ confidence intervals. Random errors were calculated by the standard methods accompanying least-squares fitting procedures (e.g., Bevington 1969; Press *et al.* 1986). In this appendix we describe the methods used to estimate bounds on the possible systematic errors.

The best kind of systematic measurement errors are those large enough to be easily recognized, and stable enough that they can be retroactively removed or allowed for. One example of such errors is a class which affects all of our TOAs to some degree, and which is particularly important when nonoverlapping data obtained with dissimilar observing systems are analyzed together. Because of widely different instrumental resolutions, a variety of receiver bandwidths, and the frequency-dependent pulse shape of PSR 1913+16, data obtained with each distinct observing system require a standard profile unique to that system. Unless simultaneous (or nearly simultaneous) observations are made, there will be unknown offsets between TOAs obtained with a given system relative to others.

Such uncalibrated offsets exist for all of our data acquired before 1978, with observing systems A–E, G, and H (see Table 1). Therefore, in solutions including these data, such as solution DD(3) discussed in § IV, additional instrumental parameters must be introduced and their values estimated along with the physically interesting parameters. One consequence is that postfit residuals and χ^2 values for these solutions will be artificially smaller than they might otherwise have been; another consequence is that the early data do not help much in determining high-precision values of the astrometric and spin parameters of the pulsar.

Residuals for the DD(3) solution are plotted as a function of date in Figure 10. Five instrumental parameters were estimated in this fit, respectively characterizing the offsets of observing systems A, B + C, D, E + G, and H. Since 1978, and especially since 1981, we have taken care to measure the offsets between TOAs obtained with different observing systems, so that additional empirical parameters would not be required. A minor exception to this rule applies to the 1983 July observations, which were carried out after some supposedly innocuous changes had been made in the equipment to permit observations of the millisecond pulsar PSR 1937+21. The single instrumental parameter included in the first seven solutions listed in Tables 4 and 5 accounts for the uncalibrated offset caused by these modifications.

More insidious systematic errors are those small enough to be individually undetectable, or with a time dependence that approximates some linear combination of terms in the model. We have taken two approaches toward allowing for possible errors of this kind. First, as described in TW, we have looked for telltale correlations among nearly adjacent postfit residuals by averaging groups of n consecutive values, and testing to see whether the standard deviations of the resulting averages decrease as $n^{-1/2}$. The results of such tests for the Mark I, Mark II, and Mark III observing systems are illustrated in Figure 11. (Similar results for the earlier observing systems were presented in Fig. 3 of TW.) With the exception of the offset in the 1983 July data mentioned earlier, we find no evidence for correlated errors in the data acquired since 1981, at least down to the 1–3 μs range.

Our second means of identifying possibly significant systematic errors concentrates on those parameters which come closest to making our "experimental design matrix" singular. For purposes of discussion, we reproduce in Table 7 the most significant portions of the normalized covariance matrix for solution DD(1). The submatrix at the top of the table includes all covariances among the astrometric and spin parameters and the single instrumental offset, O_1, while the bottom portion contains covariances among the orbital parameters and between each of them and the pulsar frequency ν. Together, these two sections include all elements of the full (15 × 15) matrix with absolute values greater than 0.3. The largest off-diagonal term is the covariance of 0.974

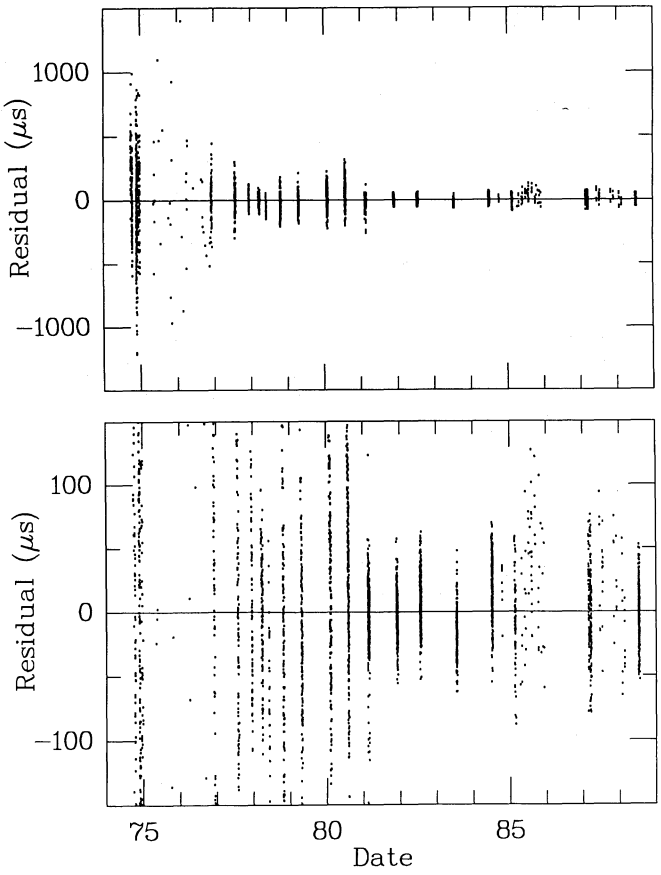

FIG. 10

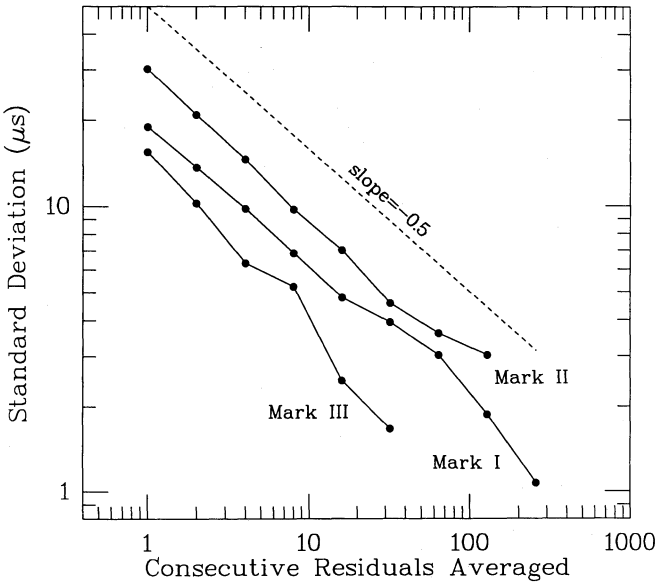

FIG. 11

FIG. 10.—Postfit residuals from the DD(3) solution, which includes all data back to 1974 with estimated uncertainties less than 500 μs. The lower panel presents the same data on a 10 times expanded vertical scale; the slight negative offset around 1983.5 illustrates the consequence of not allowing for a small instrumental offset in the 1983 July data.

FIG. 11.—Standard deviations among averages of postfit residuals obtained from sequences of consecutive measurements with the Mark I, Mark II, and Mark III systems. If the measurement errors are uncorrelated, the standard deviations should decrease as $n^{-1/2}$, as indicated by the dashed line.

TABLE 7

COVARIANCE MATRIX FOR SOLUTION DD(1)

	α	δ	μ_α	μ_δ	ν	$\dot{\nu}$	O_1
α	1.000						
δ	0.652	1.000					
μ_α	0.812	0.726	1.000				
μ_δ	0.590	0.662	0.474	1.000			
ν	−0.379	−0.505	−04.72	−0.329	1.000		
$\dot{\nu}$	0.008	0.162	0.328	−0.420	−0.346	1.000	
O_1	−0.080	0.047	−0.195	0.085	0.090	−0.420	1.000
ρ	0.863	0.918	0.905	0.916	0.969	0.905	0.610

	x	e	T_0	P_b	ω_0	$\dot{\omega}$	γ	$\dot{P}_b$
x	1.000							
e	−0.025	1.000						
T_0	−0.104	−0.009	1.000					
P_b	−0.215	−0.006	0.449	1.000				
ω_0	−0.903	0.107	0.431	0.355	1.000			
$\dot{\omega}$	−0.580	0.080	0.366	0.859	0.684	1.000		
γ	0.974	−0.207	−0.073	−0.211	−0.897	−0.584	1.000	
$\dot{P}_b$	−0.019	−0.027	−0.393	−0.186	0.035	−0.037	−0.013	1.000
ν	−0.058	−0.210	−0.206	−0.670	−0.072	−0.594	−0.013	0.075
ρ	0.991	0.839	0.957	0.952	0.992	0.983	0.994	0.819

between the parameters x and γ; these parameters become fully decoupled only on the time scale of apsidal motion, approximately 85 years.

The last row in each submatrix of Table 7 contains the "global correlation coefficient," ρ, defined as the maximum correlation between a given parameter and all possible linear combinations of the other parameters (see, for example, Eadie *et al.* 1971). The global correlation provides a relative indication of the measurability of a parameter, given the times at which measurements have been made. Values of ρ extremely close to unity indicate probable difficulties. Not surprisingly, γ has the largest global correlation, 0.994, followed by ω_0 (0.992) and x (0.991). If significant orbital phase-dependent systematic errors were present in the data, it would not be surprising to find these parameters affected by larger amounts (relative to their formal errors) than the other parameters.

The nearly random nature of the residuals in Figure 10 shows that our efforts directed toward long-term stability of the measurements have been largely successful, and that our model of the nonbinary aspects of the PSR 1913+16 system is reasonably good. On the other hand, there are some long-term (i.e., not orbit phase–dependent) systematic trends still visible in the residuals, partuclarly in the data from observing system J and, to a lesser extent, system F. For this reason the most trustworthy results from the astrometric and spin parameters, and especially their time derivatives, come from the post-1981 data.

The parameter values quoted in Table 3 were taken from solution DD(1) and a similar solution based on the CfA ephemeris. The quoted uncertainties for all parameters except $\ddot{\nu}$, $\ddot{P}$, μ_α, and μ_δ are 2–3 times the formal errors, and reflect our estimates of the largest systematic errors that might have escaped notice through the tests outlined above. The quoted uncertainties for the remaining parameters in Table 3 are 6–10 times the formal errors, and allow for the contingencies that (1) some of the uncalibrated offsets could be real and (2) timing noise and improperly calibrated offsets may have affected the proper-motion values.

For the orbital parameters as well, the most reliable solutions are based on the post-1981 data. As can be seen in the top panel of Figure 2, these observations were obtained in seven concentrated sessions each of about 2 weeks duration, plus some scattered measurements made with the Mark II system from late 1984 through early 1988. To test for the presence of session-dependent errors and their effect on the measured parameters, we carried out eight solutions similar to DD(1) except that the data from each block, in turn, was given zero weight. Except for the 1983 July offset already mentioned, this procedure brought to light no further evidence of systematic errors—and, in particular, no evidence for orbital phase-dependent errors. In these solutions even the values of γ, ω_0, and x, which have the largest global correlation coefficients, varied by no more than the uncertainties quoted in Tables 4 and 5, which are twice the formal standard errors.

Solutions carried out using the DD model require explicit assumptions for the values of δ_r, δ_θ, A, and B in equations (8) and (11). In the theory-independent phenomenological approach of §§ IV and V, the values of these parameters cannot be specified *a priori*, and yet they are too small to be measured from the existing data. In order to test the sensitivity of other parameters to the values assumed for the four small quantities, we carried out a series of solutions in which each of the first three, in turn, was first taken to have its value in general relativity given by equations (22)–(25), and then 50% larger and 50% smaller values. Similarly, B was taken to have the values 0 and $\pm 50\%$ smaller values. Similarly, B was taken to have the values 0 and $\pm 50\%$ of the nominal value of A. The χ^2 values of these fits were nearly identical (the extremes differing by less than 0.5 out of 2552), and variations in the fitted parameters were never as much as twice the uncertainties quoted in Tables 4 and 5.

REFERENCES

Backer, D. C., Fomalont, E. B., Goss, W. M., Taylor, J. H., and Weisberg, J. M. 1985, *A.J.*, **90**, 2275.
Backer, D. C., and Hellings, R. W. 1986, *Ann. Rev. Astr. Ap.*, **24**, 537.
Bailes, M. 1988, *Astr. Ap.*, **202**, 109.
Barker, B. M., and O'Connell, R. R. 1975, *Ap. J. (Letters)*, **199**, L25.
Bartel, N., Capallo, R. J., Ratner, M. I., Rogers, A. E. E., Shapiro, I. I., and Whitney, A. R. 1985, *A.J.*, **90**, 318.
Bertotti, B., Carr, B. J., and Rees, M. J. 1983, *M.N.R.A.S.*, **203**, 945.
Bevington, P. R. 1969, *Data Reduction and Error Analysis for the Physical Sciences* (New York: McGraw-Hill).
Blanchet, L., and Damour, T. 1989, *Phys. Rev.*, in press.
Blanchet, L., and Schäfer, G. 1989, *M.N.R.A.S.*, in press.
Blandford, R. D., and Teukolsky, S. A. 1976, *Ap. J.*, **205**, 580 (BT).
Boeshaar, P. C., Tyson, J. A., Pildis, R. A., and Wenk, R. A. 1988, *Bull. AAS*, **20**, 1048.
Boriakoff, V. 1973, Ph.D. thesis, Cornell University.
Burrows, A., and Woosley, S. P. 1986, *Ap. J.*, **308**, 680.
Cordes, J. M., and Downs, G. S. 1985, *Ap. J. Suppl.*, **59**, 343.
Cordes, J. M., and Wasserman, I. 1984, *Ap. J.*, **279**, 798.
Crane, P., Nelson, J. E., and Tyson, J. A. 1979, *Nature*, **280**, 367.
Damour, T. 1987, in *Gravitation in Astrophysics*, ed. B. Carter and J. B. Hartle (New York: Plenum), p. 3.
———. 1988, in *Proc. Second Canadian Conf. on General Relativity and Relativistic Astrophysics*, ed. A. Coley, C. Dyer, and T. Tupper (Singapore: World Scientific), p. 315.
Damour, T., and Deruelle, N. 1985, *Ann. Inst. H. Poincaré (Phys. Théorique)*, **43**, 107.
———. 1986, *Ann. Inst. H. Poincaré (Phys. Théorique)*, **44**, 263 (DD).
Damour, T., Gibbons, G. W., and Taylor, J. H. 1988, *Phys. Rev. Letters*, **61**, 1151.
Damour, T., and Ruffini, R. 1974, *C.R. Acad. Sci., Paris*, **279**, A971.
Damour, T., and Schäfer, G. 1988, *Nuovo Cimento*, **B101**, 127.
Damour, T., and Taylor, J. H. 1989, in preparation.
Davis, M. M., Taylor, J. H., Weisberg, J. M., and Backer, D. C. 1985, *Nature*, **315**, 547.
Eadie, W. T., Drijard, D., James, F. E., Roos, M., and Sadoulet, B. 1971, *Statistical Methods in Experimental Physics* (Amsterdam: North-Holland).
Einstein, A. 1918, *Preuss. Akad. Wiss. Sitzber. Berlin*, 154.
Elliott, K. H., Peterson, B. A., Wallace, P. T., Jones, D. H. P., Clements, E. D., Hartley, K. F., and Manchester, R. N. 1980, *M.N.R.A.S.*, **192**, 51P.
Epstein, R. 1977, *Ap. J.*, **216**, 92.
———. 1979, *Ap. J.*, **231**, 644.
Esposito, L. W., and Harrison, E. R. 1975, *Ap. J. (Letters)*, **196**, L1.
Fairhead, L., Bretagnon, P., and Lestrade, J.-F. 1988, in *The Earth's Rotation and Reference Frames for Geodesy and Geodynamics*, ed. A. K. Babcock and G. A. Wilkins (Dordrecht: Kluwer), p. 419.
Haugan, M. P. 1985, *Ap. J.*, **296**, 1.
———. 1988, preprint (H88).
Hellings, R. W., Adams, P. J., Anderson, J. D., Keesey, M. S., Lau, E. L., and Standish, E. M. 1983, *Phys. Rev. Letters*, **51**, 1609.
Hulse, R. A., and Taylor, J. H. 1975, *Ap. J. (Letters)*, **195**, L51.
Hunt, G. C., 1971, *M.N.R.A.S.*, **153**, 119.
Landau, L. D., and Lifshitz, E. M. 1962, *The Classical Theory of Fields* (Reading, MA: Addison-Wesley), p. 366.
Lyne, A. G., and Ritchings, R. T. 1977, *Nature*, **268**, 606.
Manchester, R. N., and Peters, W. 1972, *Ap. J.*, **173**, 221.
Manchester, R. N., and Taylor, J. H. 1977, *Pulsars* (San Francisco: Freeman).
Manchester, R. N., Taylor, J. H., and Van, Y. Y. 1974, *Ap. J. (Letters)*, **189**, L119.
Orsten, G. S. F. 1970, *Rev. Sci. Instr.*, **41**, 957.
Peters, P. C., and Mathews, J. 1963, *Phys. Rev.*, **131**, 435.
Press, W. H., Flannery, B. P., Teukolsky, S. A., and Vetterling, W. T. 1986, *Numerical Recipes* (Cambridge: Cambridge University Press).
Prózsyński, M. 1984, in *Millisecond Pulsars*, ed. S. P. Reynolds and D. R. Stinebring (Green Bank: NRAO), p. 287.
Rawley, L. A. 1986, Ph.D. thesis, Princeton University.
Rawley, L. A., Taylor, J. H., and Davis, M. M. 1988, *Ap. J.*, **326**, 947.
Rawley, L. A., Taylor, J. H., Davis, M. M., and Allan, D. W. 1987, *Science*. **238**, 761.
Reasenberg, R. D. 1983, *Phil. Trans. Roy. Soc. London, A*, **310**, 227.
Shapiro, I. I. 1964, *Phys. Rev. Letters*, **13**, 798.
Shapiro, S. L., and Terzian, Y. 1976, *Astr. Ap.*, **52**, 115.
Smarr, L. L., and Blandford, R. 1976, *Ap. J.*, **207**, 574.
Srinivasan, G., and van den Heuvel, E. P. J. 1982, *Astr. Ap.*, **108**, 143.

Standish, E. M. 1982, *Astr. Ap.*, **114**, 297.
Taylor, J. H. 1987, in *General Relativity and Gravitation*, ed. M. A. H. MacCallum (Cambridge: Cambridge University Press), p. 209.
———. 1989, in *Proc. NATO Advanced Study Institute, Timing Neutron Stars*, ed. H. Ögelman and E. P. J. van den Heuvel, (Dordrecht: Kluwer), p. 17.
Taylor, J. H., Fowler, L. A., and McCulloch, P. M. 1979, *Nature*, **277**, 437.
Taylor, J. H., Hulse, R. A., Fowler, L. A., Gullahorn, G. E., and Rankin, J. M. 1976, *Ap. J.* (*Letters*), **206**, L53.
Taylor, J. H., and Manchester, R. N. 1981, *A.J.*, **86**, 1953.
Taylor, J. H., and Weisberg, J. M. 1982, *Ap. J.*, **253**, 908 (TW).
van den Heuvel, E. P. J. 1987, in *The Origin and Evolution of Neutron Stars*, ed. D. J. Helfand and J.-H. Huang (Dordrecht: Reidel), p. 393.
Wagoner, R. V. 1975, *Ap. J.* (*Letters*), **196**, L63.
Wagoner, R. V., and Will, C. M. 1976, *Ap. J.*, **210**, 764.
Webbink, R. F. 1975, *Astr. Ap.*, **41**, 1.
Weisberg, J. M., Romani, R. W., and Taylor, J. H. 1989, *Ap. J.*, in press.
Weisberg, J. M., and Taylor, J. H. 1981, *Gen. Rel. Grav.*, **13**, 1.
———. 1984, *Phys. Rev. Letters*, **52**, 1348.
Will, C. M. 1981, *Theory and Experiment in Gravitational Physics* (Cambridge: Cambridge University Press).
———. 1986, *Canadian J. Phys.*, **64**, 140.

J. H. TAYLOR: Physics Department, Princeton University, Princeton, NJ 08544

J. M. WEISBERG: Department of Physics and Astronomy, Carleton College, Northfield, MN 55057